JOURNAL OF MATERIALS SCIENCE **39** (2004) 3003–3013

Nano-sized beads and porous fiber constructs of Poly(ε-caprolactone) produced by electrospinning

CHEN-MING HSU, S. SHIVKUMAR*
Department of Mechanical Engineering, Worcester Polytechnic Institute, 100 Institute Road, Worcester, MA 01609, USA
E-mail: shivkuma@wpi.edu

Nano-sized beads and non-woven porous fiber constructs of poly(ε-caprolactone) were produced by electrospinning. Nearly spherical beads with diameters between 900 nm and 5 μm were produced with dilute solutions with less than 3 wt% PCL. In this case, the initial jet of solution may split into many mini jets almost at the end of the needle and each minijet gradually disintegrates into small droplets. Beyond a critical solution concentration of about 4 wt% PCL, the jet may undergo extensional flow, splitting and splaying to produce a web of interconnected fibers with mean diameters on the order of 300 to 900 nm. Intermolecular entanglements play a dominant role in stabilizing the fibrous structure. A uniform fibrous structure was obtained at 40 kV while at 20 kV a large fraction of beads were present in the electrospun polymer. The fiber diameter in the PCL deposited on the collector typically exhibits a bimodal distribution. Electrospinning lowers the degree of crystallinity in the polymer.

1. Introduction

Porous polymers are used extensively in many applications including medical textiles, wound dressings, drug delivery devices and tissue engineering scaffolds [1]. The microstructure in these materials ranges from isolated open-pore structures to fibrous matrices. Biodegradable polymers such as poly lactic acid (PLA), poly glycolic acid (PGA), poly(ε-caprolactone) (PCL), and their copolymers and non-biodegradable polymers such as nylon, Teflon and Dacron have been the primary materials used in these applications [2]. Various techniques including phase separation, freeze drying, particle leaching and solid free form fabrication have been used to produce porous polymeric constructs for biomedical applications. In general, the typical thickness of the cell walls in the polymer and the average diameter of the ensuing porosity attainable with these techniques are on the order of 5 to 50 μm [3]. The maximum porosities obtained are often limited to about 80%. The production of porous samples with some of these techniques may be time consuming and require sophisticated equipment. Electrospinning of porous structures directly from polymer solutions may be used to overcome some of the drawbacks of the techniques outlined above [4]. Electrospinning is a technique wherein high voltages are applied to a polymer solution to produce porous structures of varying morphologies. If a dilute polymer solution is used, sub-micron sized particles of the polymer can be obtained. At high polymer concentrations in the solution, an interconnected membrane structure with a web of sub-micron fibers, may be obtained. This novel technique provides the capability of integrating various types of polymers, fibers and particles to produce unique porous materials with a structural scale on the order of nm [5]. In biomedical applications, drugs, growth factors and/or biomolecules can be incorporated into the solution so that they can be distributed uniformly in the porous structure, thereby enabling zero order release at the targeted site [6]. A wide range of pore architectures can be obtained in electrospun products. In addition, electrospun layers can also be sprayed directly onto 3-D forms, similar to painting of automotive bodies. Electrospun porous structures and fibers are being considered for many applications including protective clothing, drug delivery systems, would dressings, vascular grafts and tissue engineering scaffolds. Currently, there are over 40 synthetic or natural polymers which have been electrospun, with research focusing on the structure and morphology of electrospun polymer [7]. All these advantages have generated considerable interest in electrospinning. A variety of biopolymers including PEO, PVA, collagen and silk have been used to study the characteristics of porous structures produced by electrospinning [8–10]. The objectives of the present work are to: (a) use electrospinning as a processing technique to produce non-woven structures of PCL and (b) to characterize the physical morphology in the electrospun polymer. The effects of process variables such as applied voltage and solution concentration on the structure have been studied.

*Author to whom all correspondence should be addressed.

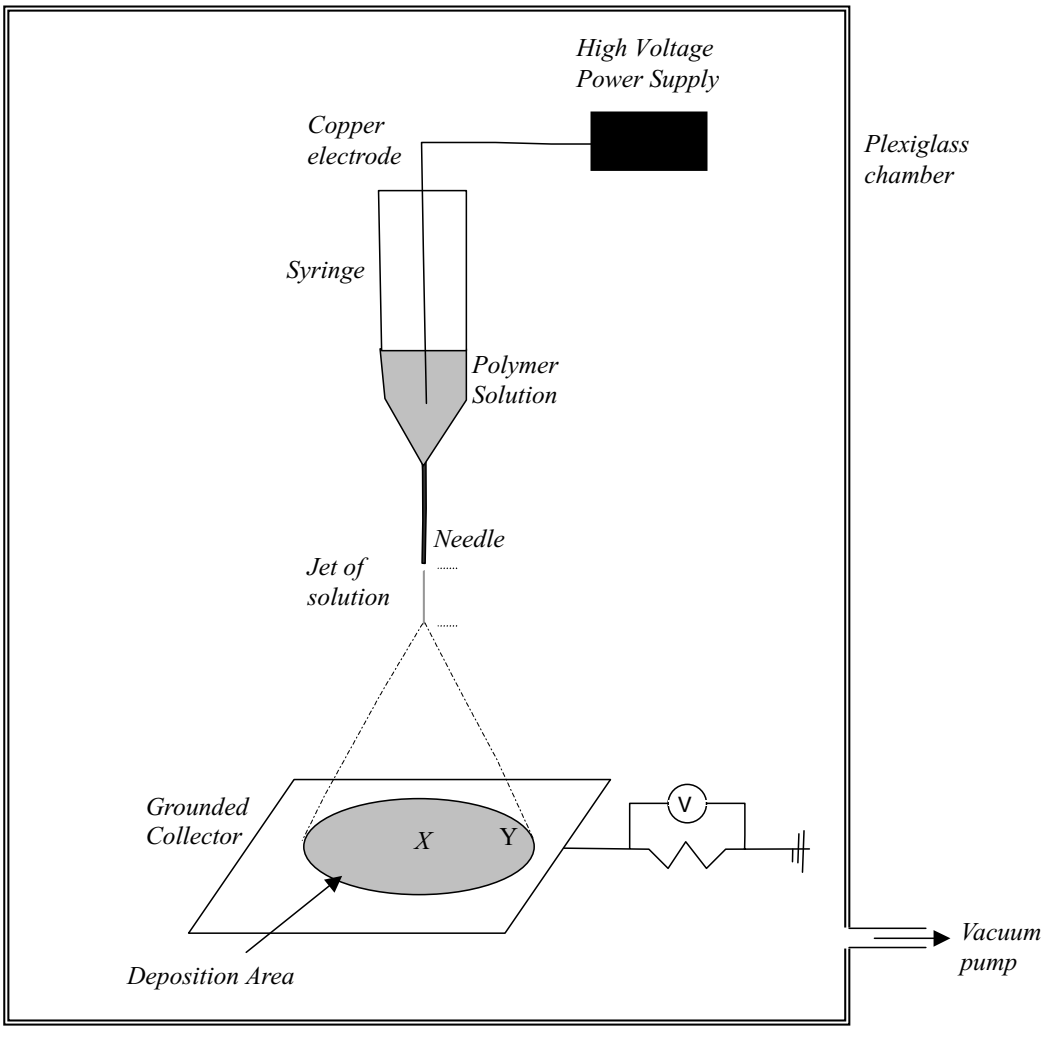

Figure 1 Schematic of the experimental set-up. Most samples for microscopic examination were obtained from the center (X) of the deposition area. Some samples were also obtained from the periphery of the deposition cone (Y).

2. Materials and methods

Poly(ε-caprolactone) (TONE Polymer 767) with a weight average molecular weight of 40,000 g/mol was obtained from Union Carbide Corporation. Danbury, CT. Analytical grade (Sigma) chloroform was used as the solvent to dissolve the PCL. A schematic of the electrospinning apparatus is shown in Fig. 1 [11]. A solution of the desired concentration of PCL was poured into a 20 ml syringe, typically equipped with 20 gage needle (Inner diameter = 0.58 mm, 39 mm long). The flow rate of the solution through the metal capillary was controlled to be on the order of 0.1 ml/min. A copper wire was inserted into the syringe and used to connect to the high voltage power supply (CPS-60 K02v1, Chungpa EMT, Co., Korea). A copper mesh (100 mm $\times$ 100 mm) with aluminum foil on top was used as the grounded collector. The syringe and the grounded collector were enclosed in a plexiglass chamber. Experiments were conducted at applied voltages between 20 and 40 kV and for solution concentrations between 1 and 9 wt%. Specimens for microscopic examination were generally obtained from the central portions (position X in Fig. 1) of the deposited deposition cone. A sample 5 mm $\times$ 5 mm in cross section was cut from the central portion. In some samples, the morphology at the periphery of the deposition cone (position Y in Fig. 1) was also examined. The cut specimens were mounted on aluminum stubs, sputter-coated with gold-palladium and examined in a JSM-840 scanning electron microscope. The images from the scanning electron microscope were analyzed with *Micosun 2000/s* image analysis software to obtain data on the distribution of particles and fibers obtained in the electrospun PCL. At least three images at various locations in the electrospun polymer were analyzed under each condition. The total number of fibers, whose diameters were measured, was typically between 80 and 100. High speed digital photography was used to study the physical phenomena occurring during electrospinning. A sony camera (DCR-TRV900) that can acquire images at the rate of 30 frames/s was positioned outside the chamber so as to record the transit of the polymer from the capillary to the grounded collector plate. The *Avid* software was used to analyze the images. Differential scanning calorimetry (DSC) was used to study the physical properties of the electrospun polymer. The samples were tested in a Perkin-Elmer DSC-7 analyzer at a heating rate of 10°C/min. The glass transition temperature, melting temperature and the degree of crystallinity in the sample were calculated from the DSC data.

3. Results and discussion

The various morphologies that can be obtained in the electrospun polymer are shown in Fig. 2. Nearly spherical beads can be produced by electrospinning of dilute polymeric solutions (Fig. 2a. If the solvent does not evaporate completely before the spherical beads reach the collector, some of the particles can agglomerate. The breakdown of the jet into droplets may be favored at low molecular weights in the polymer and at low concentrations in the solution [10]. Both solid and porous beads can be obtained depending on the processing conditions (Fig. 3). Solid beads were generally obtained at relatively low rates of solvent evaporation and small deposition distances (i.e., distance from the tip of the needle to the collector). The solvent evaporation rate could be adjusted by controlling the extent of forced convection in the plexiglass chamber (Fig. 1). By comparison, hollow beads were typically observed at high solvent evaporation rates and large deposition distances. The formation of hollow beads may be explained as follows. Rapid solvent evaporation from a drop of solution may lead to the development of a thin skin of polymer on the surface. This skin layer reduces the rate of evaporation of the solvent because of diffusional barriers. When the organic solvent inside the bead finally escapes, the atmospheric pressure tends to collapse the particle. As a result, cavities are formed on the surface of the particle.

If extensive chain entanglements exist between the polymer molecules in the solution, the jet emerging from the Taylor's cone is stabilized and the fibrous structure shown in Fig. 2b is observed. High polymer molecular weights and solution concentrations can generally stabilize the fibrous structure. Two basic fiber morphologies were observed in the electrospun samples as shown in Fig. 4. In the first case, the fibers were generally straight (indicating significant elongational flow) with a round cross section. These fibers are typically observed when the solvent has evaporated completely before reaching the collector. A wide distribution may be observed in the fiber diameter. Flat fibrous structures (Fig. 4b) are obtained with wet fibers when the solvent has not evaporated completely. The round wet fibers may flatten upon impact on the collector. The wet fibers may also undergo redissolution and coalescence as indicated by the large size of the fibers in Fig. 4b. An interesting combination of round and flat fibers can be produced by controlling the solvent evaporation rate. The surface of thick fibers exhibits a characteristic waviness as shown in Fig. 5. These surface undulations may lead to instabilities in the jet which may promote splitting and branching. By comparison, thin fibers do not exhibit these surface patterns and are relatively uniform (Fig. 5b). These fibers may have undergone repeated reductions in diameter through various processes associated with jet breakdown and may also have experienced significant extensional flow, which may eliminate the surface perturbations.

The formation of a fibrous structure in the electrospun polymer can be analyzed in terms of the breakdown of the jet under the action of an applied field. Three major types of jet breakdown were identified as

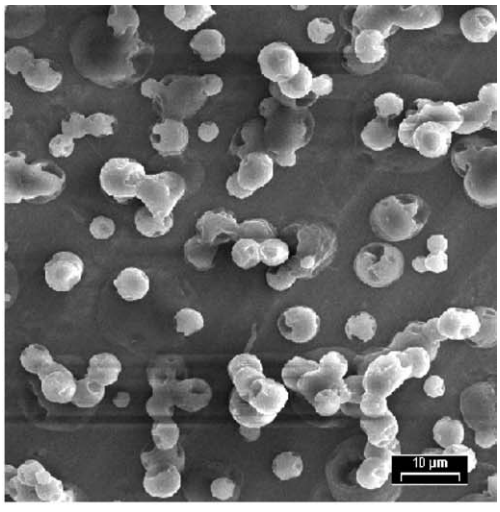

(a)

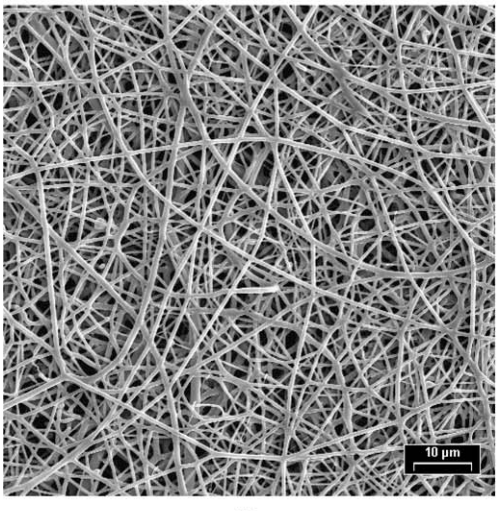

(b)

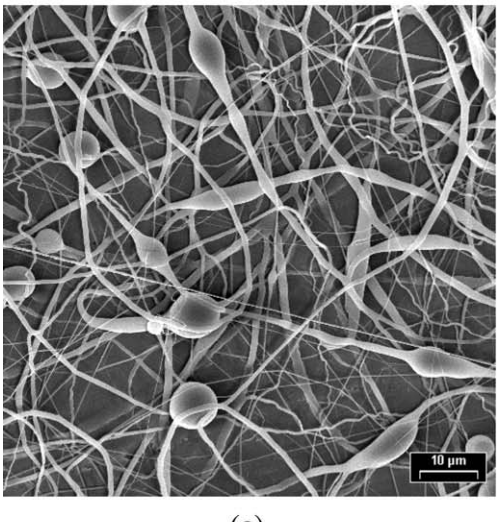

(c)

Figure 2 Photographs showing the range of structures that can be produced by electrospinning: (a) beads (b) fibers and (c) bead on string.

shown in Fig. 6. At low solution viscosities, the jet may split into a multitude of major jets almost at the end of the needle after the formation of the Taylor cone Fig. 6a. Each major jet can then split into smaller mini jets, with each minijet gradually disintegrating into small droplets. In this case, the electrospun polymer on the

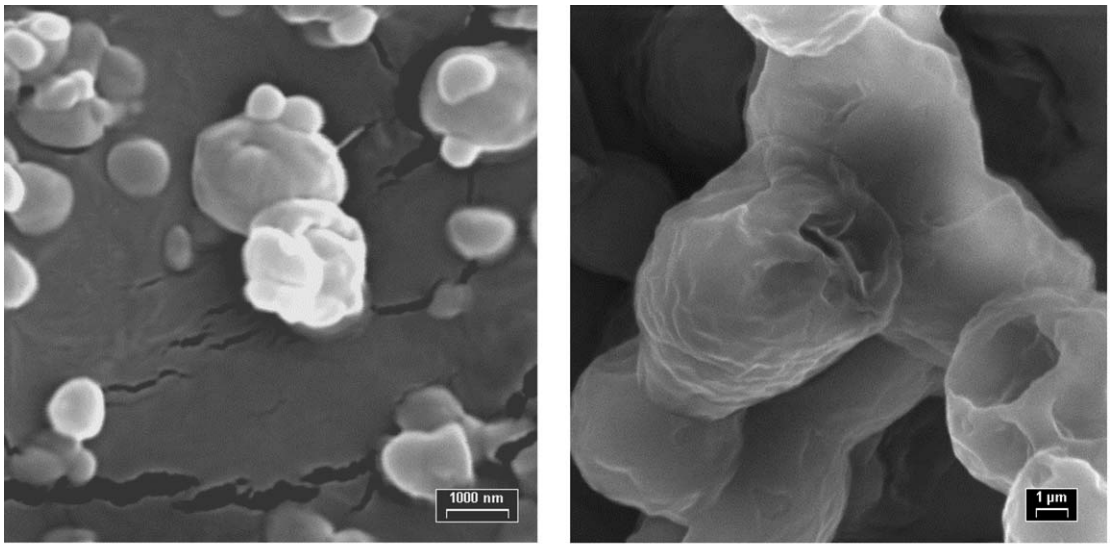

Figure 3 Photographs of: (a) solid beads and (b) porous beads produced by electrospinning.

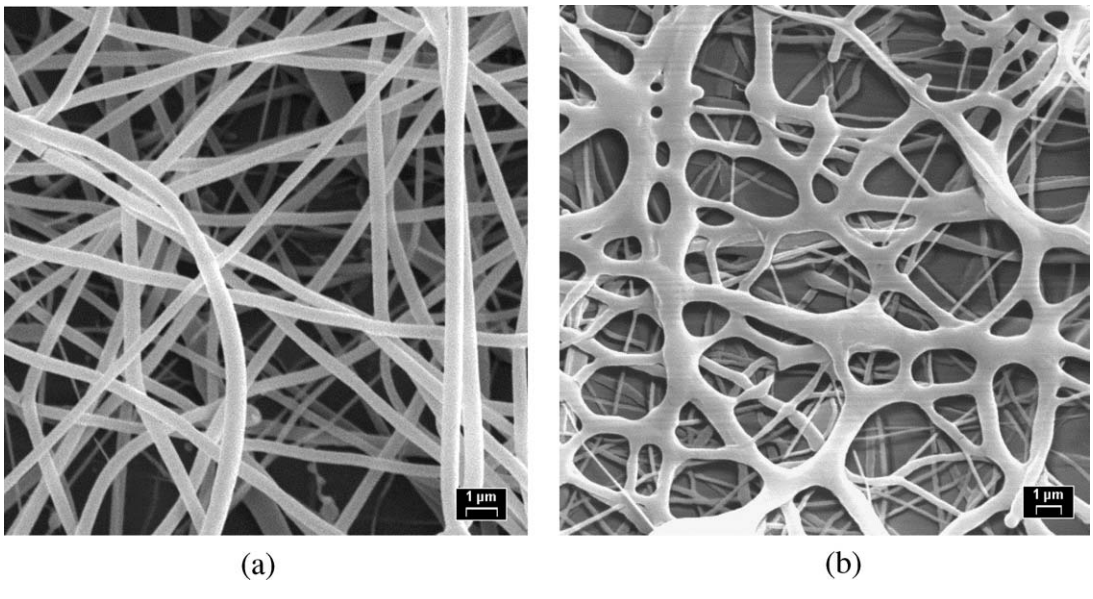

Figure 4 Photographs showing the fibrous structure in electrospun PCL. (a) The crossection of the fiber is generally circular when most of the solvent has evaporated from the jet and a dry polymer fiber is deposited on the collector plate. (b) Fiber merging and flattening is observed when wet fibers arrive at the collector.

collector will consist typically of round powders. This condition represents the sequence of events in electrospraying. In the second type of breakdown shown in Fig. 6b, the jet may again split into a multitude of major jets almost at the tip of the needle. As before, each major jet can breakdown into several mini jets, but now the mini jets are stabilized due to high viscosity. The polymer in the mini jet undergoes some extensional flow and is accelerated towards the collector. In this case, interconnected fibers may be obtained in the final sample, along with some bead-on-string structure. In the last type of breakdown shown in Fig. 6c, the jet can undergo significant elongational flow before it starts to splay. This splaying refers to the division of the primary jet into many smaller jets with almost equal diameters. The evidence of splitting and splaying can also be seen in the final polymer structure obtained on the collector. The emergence of many fibers from a bead as shown in Fig. 7 is a result of splaying. Various levels of splaying wherein 2 or more fibers may emerge from a single spherical bead may be observed in Fig. 7. An examination of the fibers obtained on the collector indicates numerous sites where they may split or splay. Examples of fiber splitting (or branching) and splaying can be seen in Fig. 8.

The structure shown in Fig. 2c, with a combination of fibers and beads is observed under many conditions. Such structures are often referred to as "bead-on-string" structures and are generally related to the instability of the jet of polymer solution [12]. The formation of beaded structures during electrospinning is fairly common and has been reported by several investigators [13]. Small beads can disassociate from the jet if the capillary instability driven by surface tension is prevented by significant viscoelastic stresses [14]. Although the exact reasons for bead formation are not clear, it has been

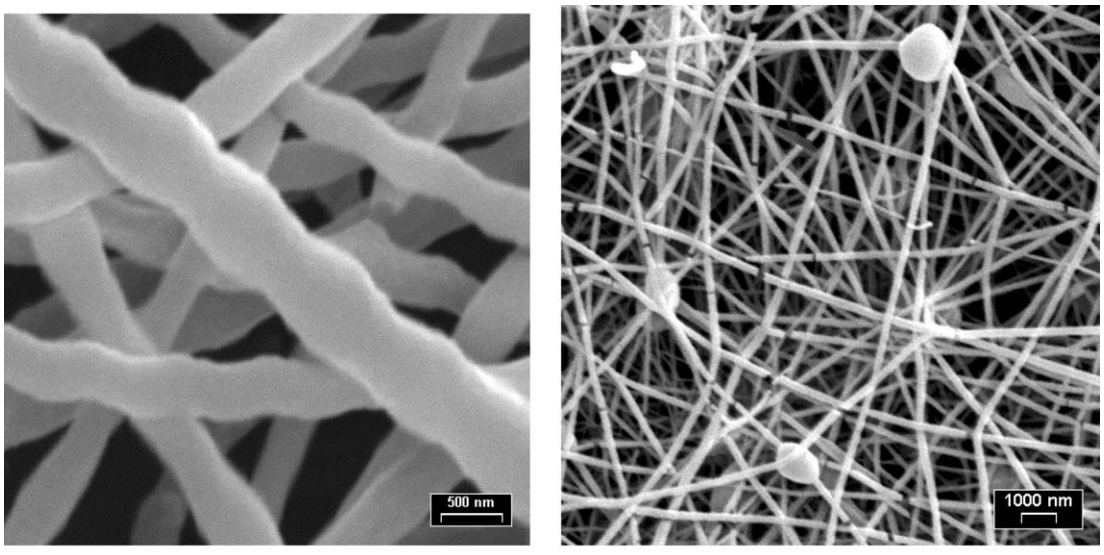

Figure 5 Photographs showing the characteristics of thick and thin fibers. (a) Thick fibers are characterized by waviness on the surface. (b) Thin fibers do not exhibit any surface waviness.

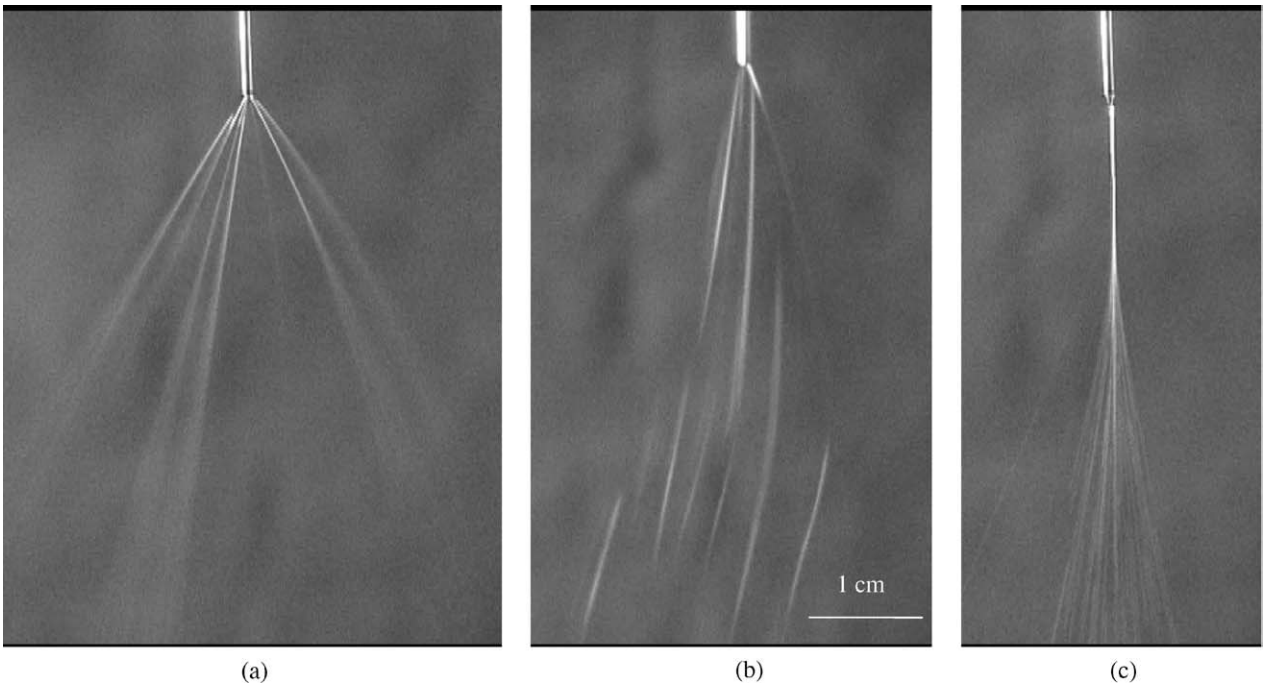

Figure 6 Photographs showing the jet breakdown for various conditions: (a) 3 wt% PCL, (b) 5 wt% PCL and (c) 7 wt% PCL.

shown that the viscoelasticity of the solution, charge density in the jet, and the surface tension of the solution are the key factors that control this behavior [13]. At low solution viscosities (i.e., low concentrations), the beads are typically spherical, while spindle-like beads are observed at high viscosities (or concentrations). A combination of round and spindle-like beads embedded in the fibers (flat and round) may be obtained under some conditions. Such structures may be especially suitable for some biomedical applications. The small fibers may provide the large surface area desired and the relatively large beads can act as reservoirs of drug or biomolecule that may enable targeted controlled release.

The solution concentration has a significant effect on the structure in the final polymer obtained on the collector. The viscosity of the solution increases with concentration and hence, the mass of PCL deposited in a given time decreases. For example, the mass of polymer deposited on the collector in 2 min was about 2.5 and 0.3 g for solution concentrations of 3 and 7 wt% PCL respectively. The deposition area also decreases with increasing concentration. The deposition areas were measured to be about 2.0 and 1.5 cm^2 for solution concentrations of 5 and 9 wt% PCL respectively. As the concentration increases, there is greater amount of elongational flow. This viscoelastic stretching may reduce the extent of spraying (or droplet formation) and thereby lower the deposition area. Typical structures in the elecstropun polymer for various concentrations are shown in Fig. 9. At solution concentrations $<1\%$ PCL, the viscosity was so low that the polymer could not be

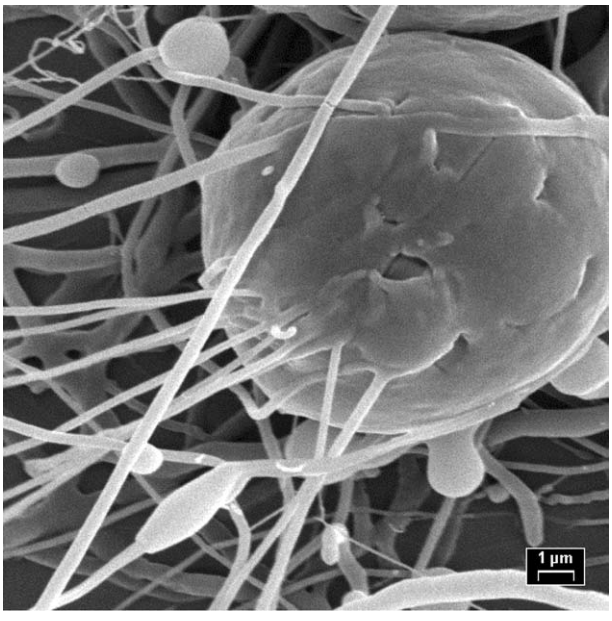

Figure 7 Photograph showing the fibers emerging from a bead.

electrosprayed or electrospun. When a 20 gage needle that was typically used with other concentrations was used, the flow rate was so rapid that the application of a voltage did not have any significant effect. So, a 26 gage (finer) needle was used with this concentration. In this case, a jet of solution of 1 wt% PCL was broken down into droplets (electrospraying) and almost spherical beads were obtained on the collector. These beads are generated by electrospraying due to the low solution viscosity. The mean size of the beads is about 900 nm as shown in shown in Fig. 10. Note that a bimodal distribution of beads was obtained (Fig. 10). Such bimodal distributions have been reported in the electrospraying literature and may result from the formation of satellite drops during jet breakdown [15]. It was observed that the sub-micron beads were generally spherical while those beads with a diameter greater than 1 μm exhibited an irregular shape. The large beads with irregular shape may be generated because of the agglomeration of small wet beads that reach the collector. Because of the low concentration, the organic solvent may not evaporate completely before the drops strike the collector, leading to surface dissolution and agglomeration. A similar behavior is observed at a solution concentration of 3 wt%, although the average particle size increases significantly as shown in Fig. 10. Note that a wide distribution of beads (with some very large beads resulting from agglomeration) is observed at a concentration of 3% (Fig. 9b). The mean size of the particles is now around 5 μm.

The transformation from beads to fibers begins at 4 wt% PCL as can be seen from Fig. 9c. In this case, small filaments between the droplets become stabilized. Finally at 5 wt% PCL, a completely fibrous interconnected structure with a web of sub-micron fibers is observed. A similar fibrous interconnected structure is also obtained at 7 wt%. When the concentration is increased to 9 wt%, the fibrous structure is not uniform, with large amounts of thick fibers and beads. A spindle-like morphology was observed in most of the beads. These results can be explained based on the viscoelastic behavior of polymer solutions. In dilute solutions, the polymer chains are sufficiently isolated and do not overlap [16]. At a critical concentration, c^*, the polymer-polymer interaction starts to become significant. At $c > c^*$, the formation of entanglements between molecules leads to a dramatic increase in viscosity. The results shown in Fig. 9 indicate that fibers start to form around 4 wt% PCL in solution indicating that entanglements are forming at this concentration. The intrinsic viscosity, $[\eta]$, for PCL can be obtained from the following equation [17]:

$$[\eta] = 9.94 \times 10^{-5} M_{\mathrm{w}}^{0.82} \tag{1}$$

Hence, the dimensionless concentration $[\eta]c$ at which the entanglements forms is $\sim$3. This value compares well with the data reported previously in other polymer systems, which indicate that chain entanglements

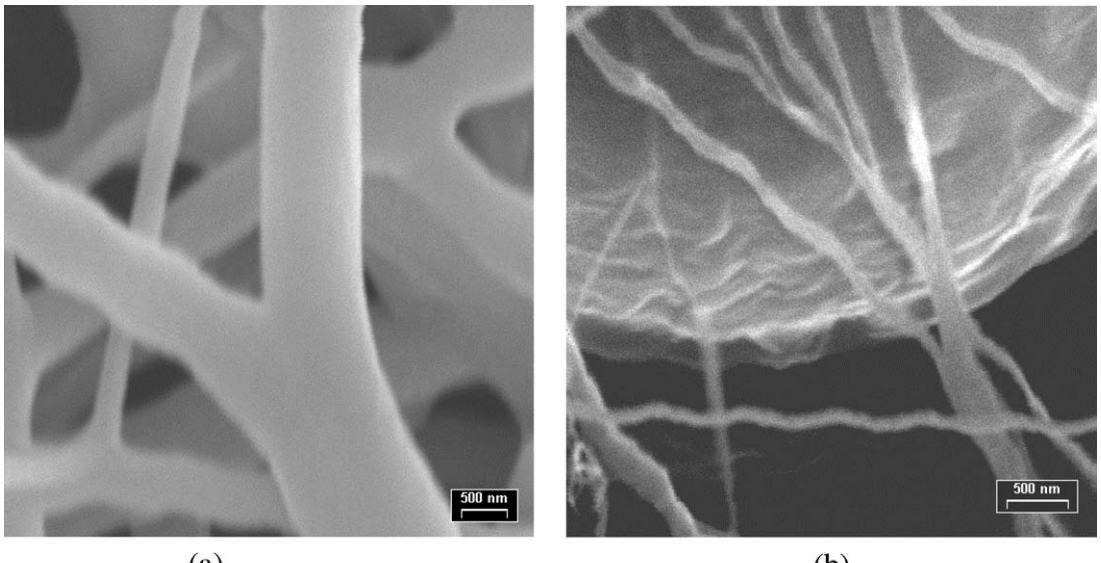

Figure 8 Photographs showing fiber: (a) splitting and (b) splaying.

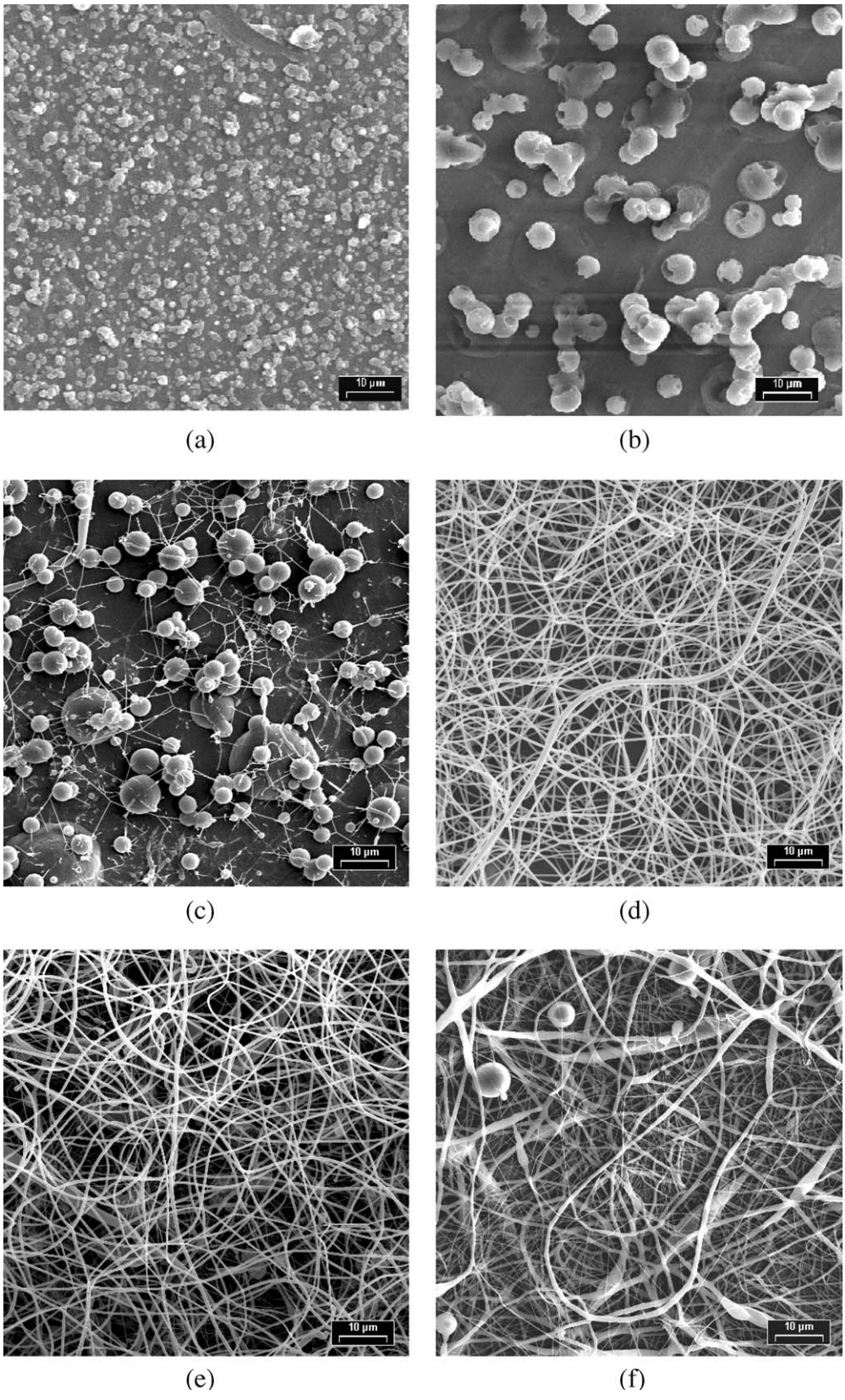

Figure 9 Photographs showing the structure of electrospun PCL for various solution concentrations: (a) 1 wt%, (b) 3 wt%, (c) 4 wt%, (d) 5 wt%, (e) 7 wt% and (f) 9 wt%.

become significant at $[\eta]c \sim 4$[18]. The best fibrous structures in this study were produced for $[\eta]c \sim 4.5$. As $[\eta]c$ is increased beyond this value, the entanglements become severe and the viscosity rises sharply. It was not possible to electrospin at concentrations greater than 9% because the viscosity was so high that the solvent evaporated before the formation of stable jet, thereby clogging the flow. Thus, there is an upper and lower limit for solution concentration during electrospinning, corresponding to the level of entanglement between the polymeric chains. This minimum and maximum concentration will depend on the molecular characteristics of the polymer (i.e., molecular weight, polydispersity, branching etc.).

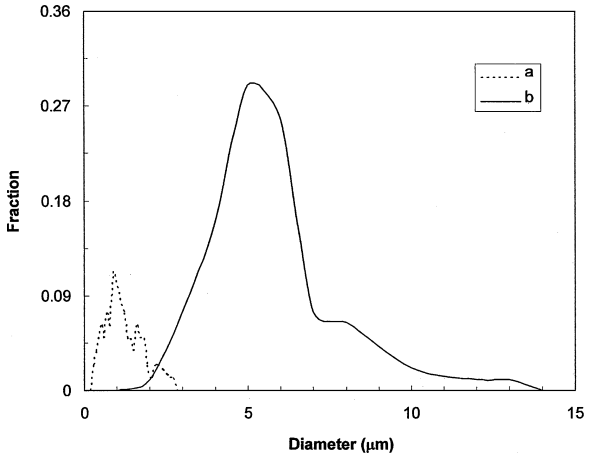

Figure 10 Bead size distribution in the polymer obtained on the collector for solution concentration of: (a) 1% PCL and (b) 3% PCL (Voltage 30 kV).

The distribution of the fibers is shown in Fig. 11. At concentrations greater than 5%, two distinct classes of fibers can be observed in the structure indicating a bimodal distribution. The mean diameters of the 1st group (smaller) and the 2nd group (bigger) are around 260 and 510 nm respectively. At 7 wt% PCL in solution, the corresponding diameters of the 2 groups are 170 and 590 nm. At 9 wt% PCL, the structure is more complicated with extensive amounts of beads and fibers, but again a bimodal distribution is observed. In this case, the mean diameters of the first group and second group are around 170 and 850 nm respectively. Further, the fraction of fibers in the 1st group was on the order of 40, 65 and 75% for 5, 7 and 9 wt% respectively. These results indicate that the diameter of the fibers in the 1st group is relatively independent of concentration, while the diameter of the fibers in the 2nd group increases with concentration. Bimodal distributions in fibers and droplets have been observed previously by many investigators [19]. The bimodal distribution may be associated with the satellite drops that may form during the breakdown of the primary jet [20]. Note for example, that a thin fiber is shooting out of a satellite drop in Fig. 12a. The diameter of this fiber is much less than other underlying fibers. A similar behavior can occur in thick fibers as shown in Fig. 12b. In addition, the splaying of the jet repeatedly to form many mini jets during its transit to the collector may also contribute to the bimodal distribution. The origin of these bimodal distributions has been linked to a transition from axisymmetric breakup to a lateral breakup of the primary jet [15].

When a voltage is applied to the solution during electrospinning, the Taylor cone is generated and at a critical voltage, a jet is ejected from the tip of the needle [21]. This critical voltage, V_c, can be calculated from the Taylor equation [22]:

$$V_c^2 = \frac{4H^2}{L^2}\left(\ln\frac{2L}{R} - \frac{3}{2}\right)(0.117\pi\gamma R) \qquad (2)$$

where H is separation distance between the needle and the collector, L is the length of the needle (or capillary), R is the radius of the needle and γ is the surface tension of the solution. The surface tension of PCL in methylene chloride has been reported be on the order of 40 mN/m [12]. Using this value in Equation 2, V_c was calculated to be 5.1 kV. It was observed experimentally that a stable jet ejected from the needle at voltages between 5.5 and 6.5 kV [11]. These values compare well with the predicted value of V_c. Note from Equation 2 that $V_c \propto \sqrt{\gamma}$, indicating that a stable jet may form at a lower voltage as γ is reduced.

The applied voltage determines the strength of the electrical field experienced in the solution and hence has a significant effect on the breakdown of the jet. Increasing the voltage generally leads to an increase in the jet current. The jet current is proportional to the

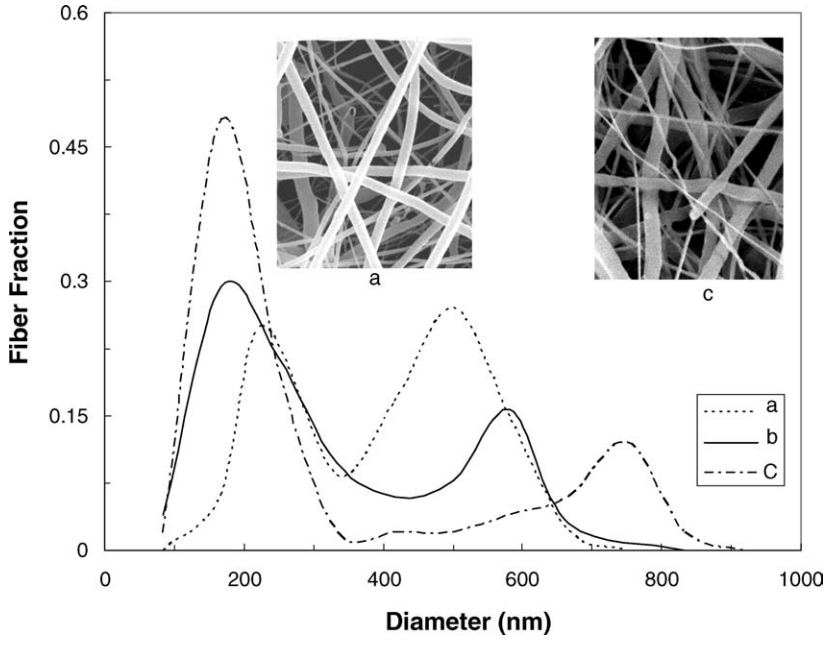

Figure 11 Fiber diameter distribution in the polymer obtained on the collector for a solution concentration of: (a) 5 wt% PCL (b) 7 wt% PCL and (c) 9 wt% PCL. The inset shows photographs of the fiber distribution for 5 wt% (a) and 9 wt% (c) (30 kV, 20 gauge needle).

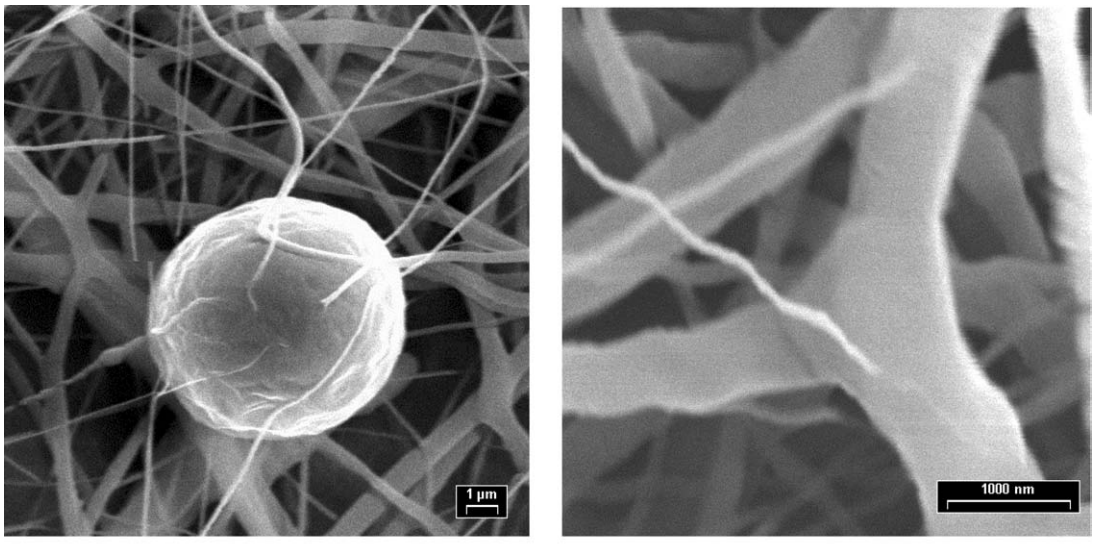

Figure 12 Photographs showing the development of thin fibers from a satellite drop (a) and from a branched fiber jet (b).

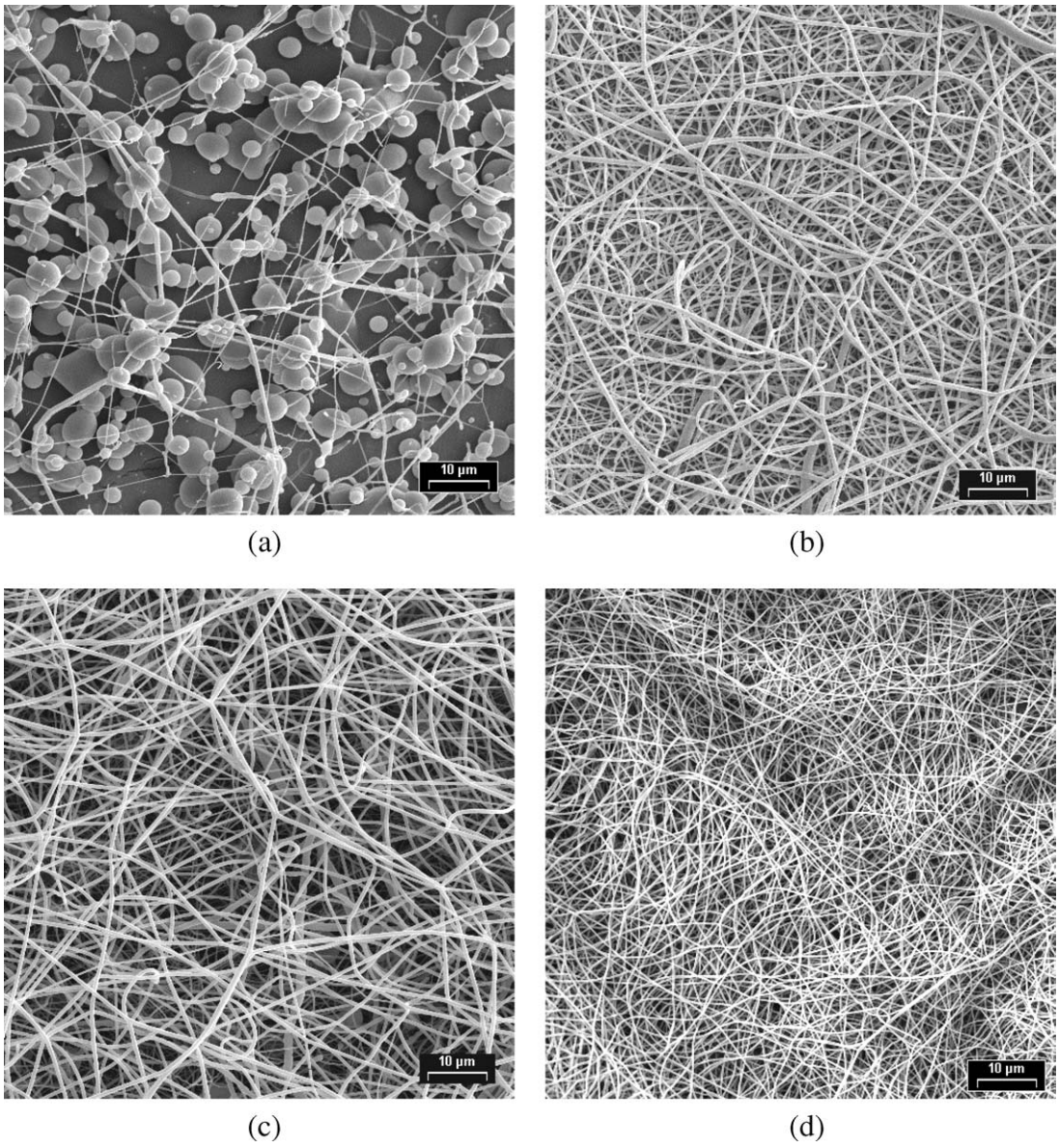

Figure 13 Photographs showing the effect of applied voltage on the structure in the electrospun polymer: (a) 20 kV, (b) 25 kV, (c) 30 kV and (d) 40 kV (solution concentration 5 wt%, deposition distance = 75 mm).

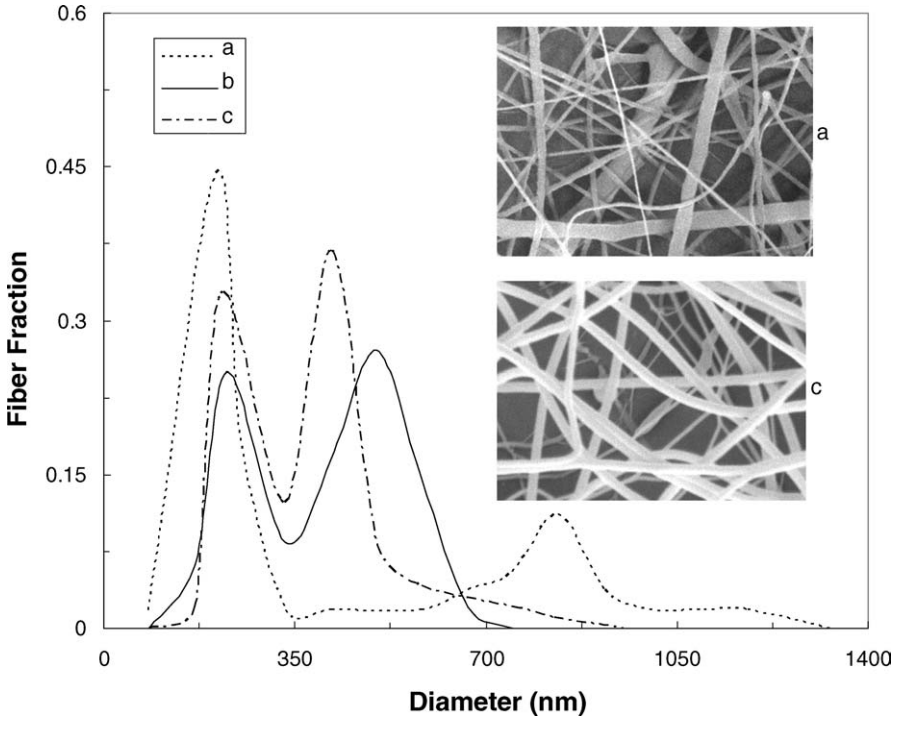

Figure 14 Fiber diameter distribution in the polymer obtained on the collector for various applied voltages: (a) 25 kV, (b) 30 kV and (c) 40 kV. The photographs in the inset show the fiber distribution at a voltage of (a) 20 kV and (c) 40 kV (concentration = 5 wt% PCL).

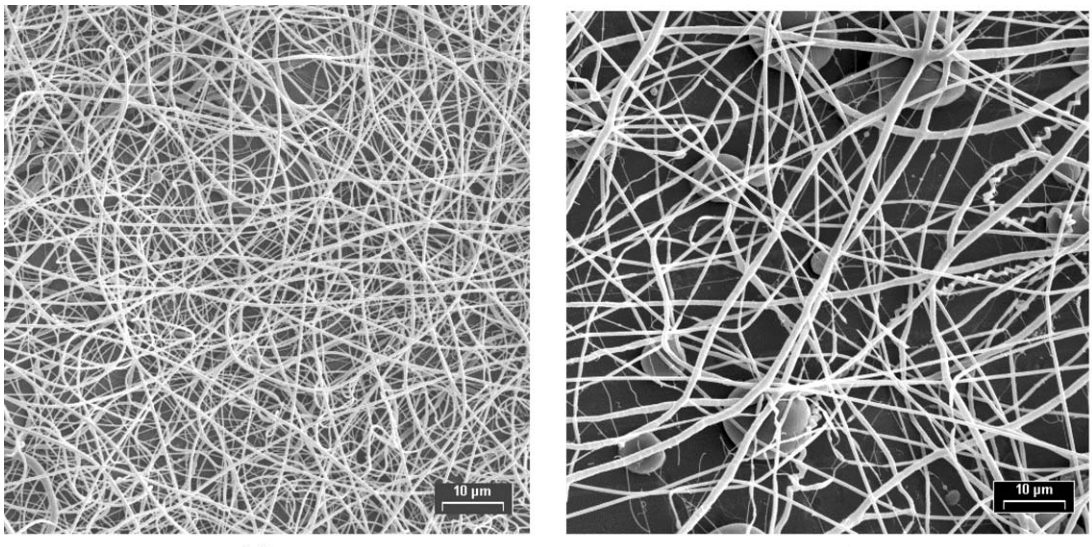

Figure 15 Photographs showing the structure at: (a) the center (X) and (b) the periphery (Y) of the deposition area (concentration = 5 wt%, Voltage = 40 kV).

transport of electrons and thus, establishes the extent of mass flow from the tip of the needle to the collector [19]. Therefore, the mass of PCL obtained on the collector increases with the applied voltage from about 0.13 g/min at 25 kV to about 0.16 g/min at 40 kV. The deposition area also increases with voltage and was measured to be on the order of 200 and 300 mm^2 at voltages 25 to 40 kV respectively. The effect of voltage on the structure in the electrospun polymer is shown in Fig. 13. At a low voltage (20 kV), the structure consists mostly of spherical beads with small filaments between the beads indicating that the bending instability is beginning to stabilize the jet. As the voltage is increased to 25 kV, a completely fibrous structure is obtained. A similar structure is also obtained at 30 kV. At 40 kV, the flow rate is so high that the fibers are packed together more densely as shown in Fig. 13d. A bimodal distribution of fibers was again observed in these samples as shown in Fig. 14. The mean diameter of the 1st group is around 260 nm for all the voltages. The mean diameter of the 2nd group in the distribution decreases with increasing voltage (430 nm at 40 kV, 510 nm at 30 kV and 670 nm at 25 kV), indicating that the splitting and splaying processes are more efficient at high voltages.

The structure in the electrospun sample varied from the centre (X) to the periphery (Y) of the deposition area (Fig. 15). Typically, the central portions contained

TABLE I %crystallinity in the electrospun polymer for various conditions. The %crystallinity was calculated from the heat of fusion (ΔH) obtained from differential scanning calorimetry. The measured heat of fusion was compared with that for fully crystalline PCL, which has been reported to be 135 J/g [23]

Condition	ΔH (J/g)	% crystallinity
As-received PCL	80	60
Electrospun PCL, 3 wt%-30 kV	45	33
Electrospun PCL, 9 wt%-30 kV	41	30
Electrospun PCL, 5 wt%-20 kV	42	31
Electrospun PCL, 5 wt%-40 kV	40	30
Electrospun PCL, 9 wt%-40 kV	47	35

a lesser number of beads, more uniform and smaller fibers than the outer portions of the deposition area. In addition, the mass deposited in the central portions (X) was also higher than on the periphery (Y), thereby producing a more compact structure as shown in Fig. 15a. This behavior can be attributed to the variations in local electrical field strength per unit length of flow. The extent of splaying is much larger at position X where the electrical field strength is much higher than at position Y, thereby leading to smaller fibers [5].

The effects of concentration and voltage on the degree of crystallinity are shown in Table I. The degree of crystallinity was calculated from DSC data. The area of the endothermic peak, typically observed at about 60°C, was compared to the heat of fusion for a completely crystalline polymer, reported to be about 135 J/g [23]. The degree of crystallinity in the base polymer before electrospinning was about 60%. The crystallinity reduces to about 30% after electrospinning. Similar results have been reported previously for other polymers [20]. After solvent evaporation, the rapid rearrangement of highly stretched chains under large elongational strains may hinder crystallinity. Solution concentration or the applied voltage did not have a significant effect on the degree of crystallinity in the electrospun polymer.

4. Conclusions

Electrospinning can be used to produce a wide range structures with poly(ε-caprolactone), PCL. The structure in the electrospun polymer may consist of beads, fibers or a combination of beads and fibers. The beads may form when the jet at the end of the Taylor's cone splits into many minijets and each minijet disintegrates into small droplets. The fibers are formed when the jet at the end of the Taylor's cone undergoes extensional flow and then disintegrates into several stable minijets that accelerate toward the collector. During its transit to the collector, each minijet can further split into smaller jets with almost equal diameter. This process known as splaying determines the size of the final fiber obtained on the collector. The solution concentration has a significant effect on the morphology of the electrospun polymer. At solution concentrations between 1 and 4 wt% PCL, the jet breaks down into droplets. The transformation from beads to interconnected fibers begins at about 4 wt% PCL in the solution. The average fiber diameter increases with solution concentration from about 510 nm at 5 wt% PCL to 850 nm at 9 wt% PCL. The fiber diameters typically exhibit a bimodal distribution. At low voltages (10 to 20 kV), the structure consists predominantly of beads with some filaments between the beads. As the voltage is increased beyond 25 kV, a fibrous structure is stabilized. The average diameter of the fiber decreases with increasing voltage. Electrospinning may lower the degree of crystallinity in the polymer.

References

1. H. HENTZE and M. ANTONIETTI, *Rev. Mol. Biotechn.* **90** (2002) 27.
2. O. PILLAI and R. PANCHAGNULA, *Curr. Opin. Chem. Biol.* **5** (2001) 447.
3. A. S. HOFFMAN, *Adv. Drug. Deliv. Rev.* **54**(1) (2002) 3.
4. E. KENAWY, J. M. LAYMAN, J. R. WATKINS, G. L. BOWLIN, J. A. MATTHEWS, D. G. SIMPSON and G. E. WNEK, *Biomaterials* **24** (2003) 907.
5. P. GIBSON, H. SCHREUDER-GIBSON and D. RIVIN, *Coll. Surf. A: Physicochem. Engng. Asp.* **187/188** (2001) 469.
6. Y. K. LUU, K. KIM, B. S. HSIAO, B. CHU and M. HADJIARGYROU, *J. Contr. Rel.* **89** (2003) 341.
7. Z. HUANG, Y. ZHANG, M. KOTAKI and S. RAMAKRISHNA, *Comp. Sci. Techn.* (2003) in press.
8. J. M. DEITZEL, J. D. KLEINMEYER, J. K. HIRVONEN and N. C. BECK TAN, *Polymer* **42** (2001) 8163.
9. K. OHGO, C. ZHAO, M. KOBAYASHI and T. ASAKURA, *ibid.* **44** (2003) 841.
10. A. KOSKI, K. YIM and S. SHIVKUMAR, *Mater. Lett.* (2003) in press.
11. CHEN-MING HSU, "Electrospinning of Poly(ε-Caprolactone)" M.S. thesis, Worcester Polytechnic Institute, Worcester, MA, 2003.
12. K. H. LEE, H. Y. KIM, M. S. KHIL, Y. M. RA and D. R. LEE, *Polymer* **44** (2003) 1287.
13. H. FONG, I. CHUN and D. H. RENEKER, *ibid.* **43** (1999) 4585.
14. R. P. MUN, J. A. BYARS and D. V. BOGER, *J. Non-Newton. Fluid Mech.* **74** (1998) 285.
15. B. KU and S. KIM, *Aerosol Sci.* **33** (2002) 1361.
16. JOEL R. FRIED, "Polymer Science and Technology" (Prentice Hall, Englewood Cliffs, NJ, 1995).
17. C. PITT, M. GRATZL, G. KIMMEL, J. SURLES and A. SCHINDLER, *Biomaterials* **2** (1981) 215.
18. P. HONG, C. CHOU and C. HE, *Polymer* **42** (2001) 6105.
19. M. M. DEMIRA, I. YILGORB, E. YILGORB and B. ERMAN, *ibid.* **43** (2002) 3303.
20. J. DEITZEL, J. KLEINMEYER, D. HARRIS and N. C. BECK TAN, *ibid.* **42** (2001) 261.
21. G. TAYLOR, *Proc. Roy. Soc. London* A **313** (1969) 453.
22. H. FONG and D. H. RENEKER, *J. Polym. Sci.: Part B: Polym. Phys.* **37** (1999) 3488.
23. G. MAGLIO, A. MIGLIOZZI and R. PALUMBO, *Polymer* **44** (2003) 369.

Received 26 August 2003
and accepted 20 January 2004